Myocardial Infarction in Mice Alters Sarcomeric Function Via Post-Translational Protein Modification

Benjamin S. Avner[1], Krystyna M. Shioura[2], Sarah B. Scruggs[1,4], David L. Geenen[2], Donald L. Helseth, Jr.[3], Mariam Farjah[1], Paul H. Goldspink[2], and R. John Solaro[1]

[1]Department of Physiology & Biophysics, [2]Department of Medicine, Section of Cardiology, [3]Chicago Biomedical Consortium/Research Resources Center Proteomics and Informatics Services Facility University of Illinois at Chicago, Chicago, IL:

[4]Departments of Physiology and Medicine, Section of Cardiology University of California at Los Angeles, Los Angeles, CA:

Address for correspondence:

R. John Solaro, PhD
Department of Physiology and Biophysics, (M/C 901)
College of Medicine
University of Illinois at Chicago
835 S. Wolcott Ave.
Chicago, Illinois 60612 –7342
Tel: 312-996-7620, Fax: 312-996-1414
Email: solarorj@uic.edu

Abstract

Myocardial physiology in the aftermath of myocardial infarction (MI) before remodeling is an under-explored area of investigation. Here, we describe the effects of MI on the cardiac sarcomere with focus on the possible contributions of reactive oxygen species (ROS). We surgically induced MI in 6-7 month old female CD1 mice by ligation of the left anterior descending coronary artery. Data were collected 3-4 days after MI or sham surgery (SH). MI hearts demonstrated ventricular dilatation and systolic dysfunction upon echo cardiographic analysis. We assessed sarcomere function *via* tension-pCa measurements of detergent extracted fiber bundles from papillary muscles. Compared to SH, Ca^{++} sensitivity was higher after MI, whereas cooperativity of activation was decreased. In experiments *in vitro*, myofibrillar protein preparations from MI ventricles showed a lower actomyosin Mg-ATPase rate associated with lower in the Ca-ATPase activity of myofilament myosin. Biochemical analysis demonstrated post-translational modification of sarcomeric proteins. Phosphorylation of cardiac troponin I (cTnI) and myosin light chain 2 was lower after MI in papillary samples, as measured using a phospho-specific stain. We identified oxidized tropomyosin after MI, forming disulfide products detectable by diagonal nonreducing-reducing SDS-PAGE. Our analysis of myocardial protein oxidation post-MI also demonstrated higher S-glutathionylation. We functionally linked protein oxidation with sarcomere function by treating skinned fibers with the sulfhydryl reducing agent dithiothreitol, which reduced Ca^{++} sensitivity in MI, but not SH, samples. Our data indicate important structural and functional alterations to the cardiac sarcomere after MI, and the contribution of protein oxidation to this process.

Key Words: myocardial infarction; reactive oxygen species; Ca-sensitivity; ATPase rate; protein phosphorylation; protein oxidation;

IntroductionHeart failure (HF) is a common endpoint of ischemic heart disease, including myocardial infarction (MI). After MI, hypertrophy of surviving cardiomyocytes combined with other remodeling effects in non-myocytes initiates the progression to clinical heart failure. Ventricular cells, including those unaffected by ischemia during the MI itself, may display altered or impaired function, a situation sometimes called "remote zone ventricular dysfunction" [1]. The physiology of the myocardium shortly after infarction when the heart has yet to begin maladaptive remodeling is therefore a clinically significant target of investigation.

Our focus in investigating cardiac physiology and pathophysiology has been the cardiac sarcomere, the basic unit of muscle contraction. Modulation of sarcomeric response to Ca^{++} is now established as a critical element in control of cardiac function [2, 3]. Sarcomeric protein modification is causal in triggering cardiac remodeling, as best exemplified by heritable cardiomyopathies caused by mutations in sarcomeric proteins [4]. Moreover, recent studies have demonstrated that post-translational modifications such as protein phosphorylation may play an important role in the progress towards the myopathy [5-7]. However, disagreement exists concerning the extent to which these changes occur in MI-induced heart failure, and the early post-MI state is relatively unexplored with regard to sarcomeric protein status.

Modulation of sarcomeric response to Ca^{++} may also involve reactive oxygen species (ROS). ROS, which include oxygen radicals such as superoxide radical ($O_2^{\bullet -}$) and hydroxyl radical ($OH^{\bullet -}$) and the non-radical reactive species hydrogen peroxide (H_2O_2), have been tied to cardiac pathophysiology for some time, with oxidation markers being closely correlated with clinical status in heart failure patients [8]. Oxidative stress is believed to be elevated in infarcted and remote regions of the post-MI heart [9, 10]. Inhibition of ROS, either through antioxidant enzyme overexpression or knockout of $O_2^{\bullet -}$-producing enzymes, appears to limit myocyte hypertrophy, contractile dysfunction and death in animal models of MI [11, 12].

In light of the failure of antioxidant vitamins such as vitamin E, which mainly affects lipid peroxidation, to prevent cardiovascular events in clinical situations [13], attention has turned to protein oxidation and other post-translational protein modifications as a mechanism of oxidation-related damage. ROS possess the

capacity to oxidize proteins directly; oxidative modifications include reversible disulfide product formation (protein disulfides or S-glutathionylation of proteins), and carbonylation. Potentially oxidized proteins in cardiac and/or skeletal muscle include actin, tropomyosin, and myosin heavy chain [14, 15]. ROS, particularly H_2O_2, are also established as signaling molecules, capable of modifying the activity of kinases and phosphatases and thus indirectly affecting the post-translational state of downstream target proteins. Numerous kinases and phosphatases are implicated as "redox sensitive" [16].

In experiments reported here, we analyzed the function and state of sarcomeric proteins function 3-4 days after experimental MI by surgical ligation of the left anterior descending (LAD) coronary artery in mice. In humans, the 72 h time point is sometimes viewed as the point of transition, at which "early" responses to MI that maintain cardiac output begin to trigger deleterious "late" remodeling, which causes myocyte hypertrophy and ventricular dilatation [17]. Our hypothesis was that at this early stage, MI induces functional alterations in the ventricular myocardium through the post-translational modification – particularly oxidation – of myofilament proteins. Our data demonstrate that MI hearts display both functional changes and post-translational myofilament protein alterations, including oxidation, and our results further implicate oxidation as a contributor to the alteration of sarcomere function.

Materials and Methods

Animals

Female CD-1 mice aged 6-7 months were purchased from Charles River Laboratories. All procedures were performed in accordance with the guidelines of the Animal Care & Use Committee of the University of Illinois at Chicago.

Murine model of MI

Surgical MI was performed [18]. Mice were anesthetized with etomidate (10 mg/kg BW; i.p.) and after intubation placed on a ventilator supplied with oxygen and 1.5% isoflurane. The heart was exteriorized and the LAD coronary artery was ligated 2 mm from the ostium with 8-0 monofilament polypropylene suture to

create MI. After the thoracotomy was closed, animals were allowed to recover on a heated pad. Sham-operated mice underwent the same procedure as described above except for the LAD ligation.

Echo cardiography

Echocardiographic examination was performed under isoflurane anesthesia with a heart rate 500-600 bpm. Anesthesia was administered with isoflurane vaporizer (SurgiVet) with 0.75-1.0% isoflurane (Halocarbon Products Corporation) delivered via nose cone and were placed in the decubitus position on a warming pad to maintain normothermia. Global and regional left ventricle (LV) function was assessed by high-resolution echo cardiography with a VeVo 770 (VisualSonics) equipped with a 30-MHz mechanical transducer 72 h after myocardial infarction (n = 6) or after sham operation (n = 4). Parasternal 2D long-axis, short-axis and four-chamber views were acquired for data analysis. Conventional echo cardiographic measurements (LV diameters, anterior and posterior wall thickness, septal wall thickness, thickening of the walls) were obtained from the M-mode images at the mid-papillary level from short-axis or long-axis views of LV and were measured according to the leading-edge method of the American Society of Echocardiography. LV end-diastolic and end-systolic volumes were calculated from the parasternal long- and short-axis views using the area-length method. Ejection fraction (EF) was calculated as EF% = (EDV-ESV)/EDV. Relative wall thickness (RWT) was calculated as the ratio of the sum of the wall thicknesses (septal and posterior) to the LVIDd. Regional wall motion index (RWMI) was used as an index of regional and global LV function and was calculated by employing the 16-segment model, where possible, or the 13-segment model. The 16-segment model is based on the scoring of the segments on three LV short-axis views (apical, mid-papillary and basal) and long axis view. The 13-segment model is based only on the basal and mid-papillary short-axis views and long-axis view. Wall motion for each segment was scored as 1 for normal, 2 for hypokinetic, 3 for akinetic and 4 for dyskinetic. The sum of scores divided by the total number of segments is RWMI.

Evans staining for visualization of perfusion and viability post-MI

Each heart was extracted and placed in cold 0.9 % NaCl. The aorta was cannulated, rinsed, and perfused with 1% Evans Blue stain. The heart was cut into 1-mm thick transverse sections using a sectioning block.

Sections were stained with 2% 2,3,5-triphenyltetrazolium chloride (TTZ) to mark viable tissue for 40 min at 37^{o}C, then placed between glass plates and fixed overnight in 10% formalin.

Functional analysis of detergent-skinned papillary muscle fibers

At 3-4 days after surgery, mice were anesthetized with pentobarbital and the hearts extracted and placed in relaxing solution (pCa 10.0). (All fiber solutions were 10 mM EGTA, 6.5 mM $MgCl_2$, 100 mM BES, 6.25 mM Na-ATP, 10 mM Na-phosphocreatine, 5 mM Na-azide, ionic strength adjusted to 0.15 M with K-propionic acid, [Ca^{++}] adjusted using $CaCl_2$ according to the computer program of Fabiato [19]). Non-infarcted left ventricular papillary muscles were removed; after papillary extraction, the remaining ventricular tissue was frozen in liquid N_2 and stored at -80^{o}C. Papillary muscles were detergent "skinned" by adding 0.5% Triton X-100 to the relaxing buffer. Skinned papillaries were further dissected into fiber bundles ~0.2 mm in diameter, and mounted between a movable rod and a force transducer. Sarcomere length was set at 2.2 μm using laser diffraction. Fiber bundles ("skinned fibers") were bathed in solutions of incrementally increasing Ca^{++} concentration, recording tension to generate tension-pCa curves (pCa = -Log [Ca^{++}]). This was repeated after treatment with 0.1 M dithiothreitol (DTT) for 10 min. Force was converted to tension by adjusting for cross-sectional area based on microscope-assisted visual estimates of diameter (3x measurements each at two different views assuming a cylindrical shape). Data were fitted to the Hill equation for non-linear regression using Prism (Graphpad).

In vitro assay of actomyosin Mg-ATPase and myosin Ca- and K-ATPase activity

We assayed actomyosin and myosin ATPase activities using the method described in [20]. For isolation of cardiac myofibrillar fractions, frozen ventricle samples were homogenized twice on ice in a Dounce homogenizer with a protein extraction buffer (60 mM KCl, 30mM imidazole, 2.5 mM $MgCl_2$, 1% Triton X-100, pH 7.0). After centrifugation, pellets were rinsed twice and re-homogenized in a rinsing buffer (60 mM KCl,, 30 mM imidazole, pH 7.0). Protein concentrations were assessed using the DC protein assay (BioRad Laboratories). Myofibrillar protein (0.25 mg/mL) was added to ATPase solution (see below) and incubated for 6 min at 30^{o}C before being mixed 1:1 with cold 10% trichloroacetic acid to stop the reaction. Pilot studies indicated that at 6 min the reaction remained linear with time. The products were developed

as follows: sample supernatant (25 µL) added to 200 µL 8.75% percholoroacetic acid, 17.5 µL 5% ammonium molybdate, 7.5 µL A.N.S. solution (3 g $NaHSO_3$, 0.6 g Na_2SO_4, 0.05 g 1-amino-2-naphthol-4-sulfonic acid per 25 mL H_2O), incubated 1 h. Absorbance was read at 655 nm. Each data point is the average of at least two replicates and is expressed as the increase in phosphate generation compared to an incubation mix stopped immediately after addition of protein. Myofibrillar proteins were incubated in parallel with four different ATPase solutions. Solutions 1 and 2 were used to assay myofilament actomyosin Mg-ATPase under relaxing (pCa ~8.0) and activating (pCa ~4.5) conditions, respectively. Solutions 3 and 4 were used to measure myofilament Ca-ATPase and K-ATPase activities, used as assays of myofilament myosin function independent of its interaction with thin filament proteins. Solution compositions were as follows:

Solution 1 – 60 mM KCl, 30 mM imidazole, 7.5 mM $MgCl_2$, 5 mM Na-ATP, 1 mM EGTA, 0.023 mM $CaCl_2$, pH 7.0

Solution 2 – 60 mM KCl, 30 mM imidazole, 7.5 mM $MgCl_2$, 5 mM Na-ATP, 1 mM EGTA, 1 mM $CaCl_2$, pH 7.0

Solution 3 – 450 mM KCl, 40 mM imidazole, 5 mM Na-ATP, 10 mM $CaCl_2$, pH 7.5

Solution 4 – 450 mM KCl, 40 mM imidazole, 5 mM Na-ATP, 10 mM EDTA, pH 7.5

Protein phosphorylation analysis

Detergent skinned papillary muscle samples were dissected as if for skinned fiber analysis, and then placed in a microtube containing 1 % SDS (10 µL per fiber bundle) and stored at -20^{o}C. To process, tubes were thawed, sonicated in a Branson Ultrasonic Cleaner at 60 Hz for 10 min, boiled 10 min, and sonicated again 10 min. Samples were combined with an equal volume 2X Gel Loading Buffer (0.125 M Tris pH 6.8, 0.4% SDS, 30% glycerol, 0.12% bromophenol blue). The resulting samples were treated with 0.1 M DTT and boiled again prior to loading onto 12% polyacrylamide gels and run using a Criterion mini-gel system. Gels were stained with ProQ Diamond Phosphoprotein Gel Stain (Invitrogen). Fluorescent scanning was performed on a Typhoon 8600 system (Molecular Dynamics). To normalize relative to total protein loading, gels were stained with Coomassie Blue stain (50% MeOH, 10% acetic acid, 0.1% Coomassie Brilliant Blue R-250 (Research Organics Inc.)). Band density was determined using ImageJ (NIH).

Western blot for site-specific phosphorylation

Protein samples were separated by SDS-PAGE as described above, then transferred in a Criterion system to a 0.2-µm thick nitrocellulose membrane for Western blot analysis. After rinsing with 1X, membranes were blocked in 1X Tris-buffered saline (TBS; 20 mM Tris-glycine, 0.08 % $NaCl_2$, pH 7.6) with 1% BSA, and then probed with a phospho-specific antibody for cardiac troponin I (cTnI) with phosphorylations at Ser 23/24 (Molecular Probes) used at 1:500. To compare to total cTnI loading, we then "stripped" the membrane with Restore Western Blot Stripping Buffer (Thermo Scientific) and re-probed with C5, an antibody to cTnI (Fitzgerald) at 1:5000. For all Western blots, the secondary antibody was either horseradish peroxidase (HRP) conjugated anti-rabbit IgG secondary antibody (Promega) used at 1:50,000 or HRP-conjugated anti-mouse IgG secondary 1:100,000 (Sigma-Aldrich). Images were developed using the ECL Plus system (Bio-Rad).

Oxidation analysis

For initial disulfide and carbonylation assays, tissue was processed and myofilament proteins extracted by processing twice in a Dounce homogenizer with 1% Triton X-100 in K-60 [60 mM KCl, 20 mM MOPS, 2 mM $MgCl_2$, 5 mM EDTA, pH 7.15], followed by two rinses and re-homogenization in a rinsing buffer (K-60 with no Triton, pH 7.15). Aliquots of the above samples were denatured in 2X Gel Loading Buffer and run on SDS-PAGE without a reducing agent. Gels were incubated in 1% DTT for 10 min, then lanes run on a second SDS-PAGE gel at a 90-degree angle to the unreduced dimension. Some diagonal gels were stained with Coomassie Blue stain; others were transferred for Western blot analysis as described above to confirm the identity of the protein of interest, tropomyosin. We used CH1, an antibody to α-tropomyosin (Developmental Studies Hybridoma Bank, University of Iowa) at a dilution of 1:500. For carbonylation analysis of myofilament protein homogenates, we employed the Oxyblot kit (Millipore) according to the manufacturer's instructions. In order to confirm initial findings in papillary samples, papillary muscle samples were prepared and processed as described above, and subjected to diagonal gel and Western blot as described.

Assessment of protein glutathionylation

Myofibrillar protein samples were prepared from frozen ventricular tissue as described above, except that 4 mM N-ethylmaleimide (NEM) was added to the K-60 buffers just prior to processing. The positive and negative controls for this experiment were created by incubating pooled samples, after denaturing, with 0.5 mM DTT (negative control) or 2 mM each reduced glutathione and diamide (Sigma-Aldrich) (positive control, as established in [21]) for 10 min at 37^{o}C. Western blots were performed as described above. We used D8, a monoclonal antibody to glutathione (AbCam) at 1:275. Ponceau S solution (Sigma) was used to visualize actin loading.

Mass spectrometry analysis (LC/MS/MS)

Diagonal gels were stained with Simply Blue Coomassie G-250 (Invitrogen) for 1 h and destained with Milli-Q H_2O. Spots were cut and placed in multiple aliquots of destain solution (100 mM NH_4HCO_3/50% acetonitrile) and dehydrated with 100% acetonitrile (AcN). Spots were rehydrated with trypsin (Promega) in 40 mM NH_4HCO_3/10% AcN at an enzyme to protein ratio of 1:50 and placed at 37ºC for 18 h. Peptides were extracted twice with 0.1% TFA/50% AcN. Extracts were pooled, concentrated, and re-solubilized in buffer A (95% H_2O/5% AcN). Protein ID was performed on an LTQ-FT (Thermo Fisher) mass spectrometer equipped with a capillary column and a nanospray ionization source. Peptides were loaded onto a C_{18} column at a flow rate of 200 nL/min, and eluted with an increasing gradient of buffer B (95% AcN/5% H_2O). High resolution MS1 scans were performed at a resolution of 50,000. MS2 CID (energy=35%) was performed in data dependent mode with the 5 most abundant ions per scan selected for fragmentation, and a dynamic exclusion time of 1 min. Tandem mass spectra were extracted, charge state deconvoluted and deisotoped by converting RAW files to mzXML using version 4.0.2 of the tool ReAdW.exe; these mzXML files were converted to MGF for submission to Mascot using the tool MsXML2Other (both tools Institute for Systems Biology, Seattle, WA). All MS/MS samples were analyzed using Mascot (Matrix Science, London, UK; version 2.2.04). Mascot was set up to search the ipi.MOUSE.v3.50 database (3.50, 55521 entries) assuming the digestion enzyme trypsin and allowing two missed cleavages. Mascot was searched with a fragment ion mass tolerance of 0.60 Da and a parent ion tolerance of 10.0 PPM. Scaffold (version Scaffold_2_06_01, Proteome Software Inc., Portland, OR) was

used to validate MS/MS based peptide and protein identifications. Peptide identifications were accepted if they could be established at greater than 90.0% probability as specified by the Peptide Prophet algorithm [22]. Protein identifications were accepted if they could be established at greater than 95.0% probability and contained at least 2 unique peptides. Protein probabilities were assigned by the Protein Prophet algorithm [23]. Proteins that contained similar peptides and could not be differentiated based on MS/MS analysis alone were grouped to satisfy the principles of parsimony: +2, +3.

Statistics

We compared SH and MI hearts using Student's t-test with $\alpha = 0.05$. Before-after comparisons of DTT treatment of skinned fibers were assessed by paired t-test with $\alpha = 0.05$. Statistical computations were performed using Prism. All numerical data are presented as mean ± standard error of the mean (SEM).

Results

Effect of MI on ventricular anatomy and function

In order to characterize ventricular function *in vivo*, we performed echo cardiography measurements 3 days after coronary ligation or sham operation to assess ventricular function. MI hearts displayed a pronounced impairment in left ventricular systolic function as assessed by higher systolic and diastolic diameters and lower fractional shortening (Figure 1A), along with wall thickening. SH vs. MI mean ± SEM for these parameters were as follows: LVIDs (mm) (2.0 ± 0.2 vs. 4.5 ± 0.3, $p < 0.0001$), LVIDd (mm) (3.3 ± 0.1 vs. 4.8 ± 0.2, $p < 0.0001$), EF (%) (71 ± 3 vs. 19 ± 3, $p < 0.0001$), RWT (0.62 ± 0.02 vs. 0.33 ± 0.01, $p < 0.0001$). The average regional wall motion index score was also significantly different (1 ± 0.0 SH, 2 ± 0.5 MI, $p < 0.0001$), indicating hypokinetic motion after MI. The cardiac output did not significantly differ between the two groups (in mL/min, 17.4 ± 2.6 SH, 12.6 ± 2.4 MI), speaking to the tendency of the heart to achieve short-term maintenance of cardiac output in pathology, often with long-term consequences [24].

Upon extraction 3-4 days after surgery, MI hearts had visible "necrotic" areas of white-yellow discoloration. A typical Evans Blue stain of the infarcted heart is shown (Figure 1B): the dark blue areas represent fully viable tissue, the red areas represent "at risk" zones that are non-perfused but viable, and the

white regions are necrotic and non-viable. A large portion of the ventricle in this representative heart is destroyed or damaged, but the basal portion of both papillary muscles and the entirety of one survived the MI. Thus, we were able to employ samples of non-infarcted papillary muscle in our investigations of sarcomeric function and sarcomeric protein state in myocardium approximating the "remote zone" of the ventricle.

After hearts were extracted for use in the experiments described below, they were weighed; the ratio of wet heart weight to body weight was significantly higher in MI hearts (mean ± SEM of mg HW/g BW ratios: 4.9 ± 0.2 SH, 6.1 ± 0.3 MI, n = 10, $p < 0.01$).

Assessment of sarcomeric function post-MI

We analyzed sarcomeric function by means of the tension-pCa relationship recorded on fiber bundles dissected from detergent "skinned" papillary muscles. [Ca^{++}] was expressed as pCa, the -log of the M Ca^{++} concentration. Force generation was measured as samples were incubated in solutions of incrementally increasing [Ca^{++}]. This "skinned fiber" technique serves as a proxy for the fundamental functional traits of the sarcomere itself, independent of the influence of cell membranes, cytosolic signaling, or Ca^{++} fluxes. All measurements on papillary muscles from MI hearts were performed on regions of tissue that were not visibly infarcted. (Infarcted muscle did not generate noticeable contractile force in response to Ca^{++}.)

Sarcomeric function differed between SH and MI samples (Table 1 and Figure 2). Ca^{++} sensitivity was significantly higher in MI samples compared to SH, as assessed by the pCa_{50} parameter. Cooperativity of activation, as measured by Hill n values, was lower in the MI group. Maximum tension generated at pCa 4.5 was not significantly different after MI. These findings characterize functional differences in the cardiac contractile machinery that are present in the surviving regions of the myocardium, which may presage or trigger the development of decompensation and heart failure.

In vitro measurements of myofibrillar ATPase activity in myofibrillar tissue from MI and sham-operated hearts

We incorporated *in vitro* assays of ATP consumption in order to elucidate any effect that MI might have on myofibrillar myosin, a protein which has been reported to be oxidized [15]. In addition to measurements of actomyosin Mg-ATPase to assess the function of interacting myofilament proteins, we also measured myosin Ca-ATPase and myosin K-ATPase, which record the enzymatic activity of myofibrillar myosin under conditions in which it does not interact with actin. Hearts were homogenized in buffer containing detergent in order to isolate the myofilament fraction. Due to the quantity of sample required in order to perform this experiment, no distinction was made between different regions of ventricular tissue, and the "MI" samples incorporated both infarcted and non-infarcted regions of myocardium.

The ATPase rates are depicted graphically (Figure 3). Actomyosin Mg-ATP hydrolysis was lower after MI under activating conditions (pCa ~4.5; in nmol PO_4/mg tissue/min, 232 ± 13 SH, 180 ± 12 MI, $p < 0.01$), but not relaxing conditions (pCa ~8.0; 53 ± 4 SH, 51 ± 4 MI), demonstrating differing actomyosin function. This is likely to be caused by an alteration in the enzymatic function of myofilament myosin, as myosin Ca-ATPase also significantly lower in MI samples (426 ± 20 SH, 336 ± 21 MI, $p < 0.005$). It is unlikely that this finding is an artifact caused by a reduction in viable myosin after infarction, inasmuch as myofilament myosin K-ATPase was similar between the SH and MI samples (107 ± 13 SH, 131 ± 120 MI) - an indication that the net amount of functional myofibrillar myosin was not lower in the MI group.

Assessment of sarcomeric protein phosphorylation levels post-MI

As alterations in protein phosphorylation are well known to influence measures of sarcomeric function, including Ca^{++} sensitivity, we analyzed net phosphorylation status in samples derived from papillary "skinned fibers." Fiber bundles from papillary muscles were collected and dissected analogously to those used for functional experiments; in MI hearts, the sample included only portions > 1 mm distant from the visibly infarcted area. After processing, the sarcomeric proteins were separated by SDS-PAGE and the gel was stained with ProQ Diamond Phosphoprotein Stain, a fluorescent dye targeting phosphorylated Ser/Thr residues on proteins.

We measured the phosphorylation level of each indicated protein as assessed by optical density after ProQ staining (Figure 4). Values are adjusted relative to lane loading by dividing by the optical density of actin after Coomassie blue staining. Phosphorylation of two proteins – cTnI and myosin light chain 2 (MLC2) – was lower after MI. Cardiac troponin I displayed ~20% less phosphorylation in MI samples (0.57 ± 0.03 SH, 0.46 ± 0.02 MI $p < 0.05$). Myosin light chain 2 was also ~20% less phosphorylated (0.15 ± 0.01 SH, 0.11 ± 0.01 MI, $p < 0.05$). We did not observe a significant difference between the two groups for phosphorylation of MyBP-C, desmin, cTnT, or Tm.

Decreases in phosphorylation at Ser 23/24 of cTnI are expected to induce an increase in Ca^{++} sensitivity. We therefore employed a phospho-specific antibody for this form of cTnI, which was adjusted relative to the signal from an antibody to total cTnI. Surprisingly, the ratio of 23/24-phospho cTnI signal to total cTnI signal was similar between the SH and MI conditions indicating that these residues are not the site of the difference in total cTnI phosphorylation observed following MI (data not shown).

Assessment of sarcomeric protein oxidation levels post-MI

We used diagonal non-reducing/reducing SDS-PAGE to detect the formation of disulfide products, an early marker of protein oxidation. In this technique, proteins were initially separated by electrophoresis under non-reducing conditions, the resulting gel was treated with a reducing agent (DTT), and SDS-PAGE was repeated at a 90^{o} angle to the original separation. Disulfide products – proteins running at a high molecular weight in the non-reducing condition and a lower molecular weight after DTT treatment – could be observed to the left of the diagonal line formed by the non-oxidized proteins.

A representative diagonal gel, containing samples derived from whole-ventricle myofibrillar extracts from an MI heart and a SH heart, is shown (Figure 5A). The circled spot appeared at the same molecular weight as Tm after reducing, indicating it to be an oxidized product of Tm. The Tm product of interest formed in MI samples and was much reduced or absent in SH samples; this difference was observed in 7 out of 8 pairings. The oxidized spot reacted with an antibody to Tm on diagonal Western blotting, and the identity

of the oxidized protein was further confirmed using LC-MS/MS (Figure 5B). We also compared protein carbonylation using the Oxyblot technique; we did not detect a difference in carbonylation between MI and SH (data not shown).

We repeated the diagonal gel experiments on non-infarcted papillary skinned fiber samples as described above in order to see if they would exhibit the same pattern as samples derived from whole ventricles. In 7 out of 9 cases, the MI sample visibly demonstrated enhanced formation of the oxidized Tm product compared to the SH.

Measures of protein glutathionylation

Protein glutathionylation as a result of the formation of mixed disulfides is another index of oxidative stress that is one of the first observed responses [25]. We therefore used Western blotting to analyze glutathione formation in order to evaluate whether sarcomeric proteins from MI hearts indeed experienced oxidative stress conditions (Figure 6). These data were collected from the sarcomeric fractions of whole-ventricle samples. The values represent optical density of the bands detected by anti-glutathione on Western blot, adjusted for loading by dividing by the optical density of actin after Ponceau S stain of the membrane. In n = 5 SH samples, 7 MI samples, glutathionylation was significantly higher after MI (0.23 ± 0.02 SH, 0.34 ± 0.03 MI, $p < 0.05$). The product appeared as a high molecular weight band, possibly representing the glutathionylation of titin. This result establishes the increase in oxidative stress and protein oxidation within the myofibrillar protein fraction in the aftermath of MI, and illustrates the novel finding of protein glutathionylation in cardiac pathophysiology.

Effect of a reducing agent on Ca^{++} sensitivity

The above results demonstrate evidence of MI-induced sarcomeric protein oxidation. In order to determine whether protein oxidation is a contributing factor to the altered sarcomeric function shown in Figure 2, we compared the Ca^{++} sensitivity of SH and MI skinned fibers before and after treatment with 0.1 M DTT. Max tension and Hill slope typically decreased between 10 and 20% for the second contraction series;

however, control experiments demonstrated that pCa_{50} remained stable across multiple tension-pCa measurements of the same skinned fiber from both SH and MI hearts (data not shown).
Reduction by DTT did not exert a significant effect on fibers from SH animals. However, the Ca^{++} sensitivity of fibers from post-MI animals was significantly lower after DTT treatment than before (Figure 7). This finding establishes a causal link between protein oxidation and a change in sarcomeric function seen following MI, since reversal of the former blunts or eliminates the latter.

Discussion

Our experimental findings characterize the relatively unexplored question of how the cardiac sarcomere is affected during the short-term aftermath of myocardial infarction. The significant findings include changes in sarcomeric function – higher Ca^{++} sensitivity of force generation and lower cooperativity of activation – and altered post-translational state of individual sarcomeric proteins, including myofibrillar myosin, MLC2, cTnI, and Tm. In addition, we present a novel description of a link between ROS-induced protein oxidation with MI-induced alterations in sarcomere function, illuminating the contributions of oxidation to the early stages of the post-MI condition.

This study contrasts with the finding by Christopher *et* al [26] of a transient decrease in Ca^{++} sensitivity after 3 days of ischemia through surgically-induced reduction in blood flow in rat hearts followed by an increase with progressing pathology. Importantly, we derived these measurements from viable non-ischemic myocardium rather than the affected ischemic myocardium. Already at this early time point we discovered an increase in Ca^{++} sensitivity and a decrease in cooperativity of activation. Ca^{++} sensitivity was also increased at a later time point (3 weeks) in a pig model of MI [27], indicating that this functional change may be common across an extended time period in small and large mammal systems. However, measurements taken from skinned rat cardiomyocytes 7 days after MI by coronary artery occlusion included a decrease in Ca^{++} sensitivity in another study [28]. By the end of the progression to end stage HF, Ca^{++} sensitivity may be decreased [29]. Cooperativity of activation, by mechanisms which are not entirely clear, is a hallmark of cardiac muscle contraction. Cooperativity underlies the steepness of the force-pCa relationship, as well as the rate of the cardiac cycle, particularly the period of force generation

postulated to continue after the fall of the Ca^{++} transient [30, 31]. Reduced cooperativity as seen in our MI samples may lead to a reduction in elastance during systole or hasten the onset of ventricular relaxation.

The finding of decreased ATPase activity in failing hearts has been known for decades in humans [32]. The present study demonstrates that this characteristic begins in the early post-MI period, and further demonstrates the contribution of a modification of myofilament myosin leading to a decrease in Ca-ATPase activity. One of the few other studies to investigate the early period following MI in mice was performed by Rao *et al* [1]. They used isolated filaments to perform i*n vitro* motility assays showing decreased velocity, and further demonstrated myosin heavy chain oxidation at reactive cysteines. Although this is certainly consistent with our finding of myosin ATPase modification, it should be noted that the differences in motility assays were observed in the presence of DTT. The authors thus concluded that at least some of this effect was not due to reducible modifications such as disulfide bond formation. Treatment with very high concentrations (50 mM) of H_2O_2 also induced functional alterations to rabbit skeletal myofibrillar myosin attributable to irreversible oxidation [15].

Total phosphorylation of cTnI and MLC2 was decreased in our MI samples. This is also observed in some but not all studies of end stage HF [2]. Our data are consistent with another recent study utilizing the same form of surgery to generate MI in mice [33]. Unlike us, these experimenters did specifically observe a decrease in cTnI Ser 23/24 phosphorylation at 2 days post-MI, which disappeared at later time points. Their article posits a series of phosphorylation changes *en route* to heart failure, including an eventual possible increase in net cTnI phosphorylation ocurring 2-4 months after MI. Interestingly, increased MLC2 phosphorylation is known to increase Ca^{++} sensitivity [34]. The current finding of Ca^{++} sensitization with reduced MLC2 phosphorylation thus represents an unexpected combination. It is possible that the individual components of the myofibrillar response to MI influence functional properties in different directions. The effect of a small but significant increase in Ca^{++} sensitivity may emerge as a net result of sensitizing and desensitizing processes. Though ROS act as signaling molecules and may indirectly affect protein phosphorylation levels, a connection between ROS levels and the changes in phospho-protein levels after MI remains speculative. In any event, phosphorylation modification cannot entirely explain the

change in Ca^{++} sensitivity given that it was blunted by DTT, the reducing agent used in preparing the samples for phospho-protein analysis. This finding is in and of itself interesting due to the documented capacity of non-failing cTn to fully abrogate the change in Ca^{++} sensitivity in myocytes from failing rat hearts [29]. We speculate thatmyofilament protein oxidation may play as important a role as phosphorylation in shaping sarcomeric function after MI.

Protein oxidation may manifest as protein S-glutathionylation through a mechanism in which a reactive sulfhydryl in a protein's Cys residue forms a mixed disulfide with glutathione. Glutathionylation has been shown to reduce the force generating ability of skeletal muscle [21], but may also be a component of ROS-based signaling, or even a protective mechanism to prevent irreversible protein damage [25]. We note that we detected an increase after MI only in reversible protein oxidation – protein disulfides and glutathione-based mixed disulfides – rather than irreversible protein carbonylation. Work in a rat model of ischemia for 1 h has also implicated actin as a potential target of glutathionylation [35]. We did not find evidence of actin glutathionylation in our analysis of glutathionylated proteins. Putatively oxidized actin-containing products could be seen on diagonal gels (Figure 5), but showed no clear pattern of difference between SH and MI samples.

Other experimenters have perfused rat hearts with H_2O_2 and observed oxidation of both actin and Tm on diagonal gels [14]. Tm oxidation is also reported in recent work utilizing a Langendorff perfusion model of ischemia-reperfusion in mouse hearts and linked to mitochondrial ROS production [36], as well as in a pacing induced HF model in rabbits [37]. In the present set of experiments, Tm was clearly oxidized to form disulfide products after MI. Given that Tm only contains one Cys residue in each chain (Cys190), we hypothesized that this product represented a Tm dimer. Our mass spectrometry analysis lends support to this idea, inasmuch as no other sarcomeric proteins were detected in the Tm spot. Specific domains of Tm, including residues 175-190, affect Ca^{++} sensitivity and myofilament function. Some familial hypertrophic cardiomyopathy mutations are characterized by a nearby Tm mutation and increased Ca^{++} sensitivity [38, 39]. Thus, there is precedent for linking modification of this specific region of Tm with higher Ca^{++} sensitivity, although this is not a universal effect [40]. Residues 175-190 are believed to comprise a

binding site for cTnT, suggesting that an alteration in this interaction could impact the series of signals that allow the Tn complex to respond to Ca^{++} binding by moving Tm on actin.

We demonstrated the functional relevance of our findings related to protein oxidation through our data showing that the change in Ca^{++} sensitivity induced by MI could be reversed by a reducing agent. To our knowledge, this is the first investigation of cardiac pathology to incorporate a reducing agent to in this manner to link protein oxidation with sarcomeric function. The antagonistic action of one ROS (H_2O_2) and DTT was previously reported, with each capable of completely reversing the impairment of force generation by the other in (unskinned) mouse skeletal muscle preparations [41]. However, these authors attribute the effects to perturbations in cellular redox balance rather than modification of myofilaments. In these systems DTT caused a decrease in Ca^{++} sensitivity, whereas it did not noticeably alter the control preparations of the present study. Bucillamine, a dithiol-based antioxidant which works by maintaining a reducing environment in the cell, prevented loss of cardiac function after temporary LAD ligation in mice [42], although the authors of that study did not investigate post-translational protein modification.

When assessing the effect of any process that occurs following a pathophysiological stress, one cannot definitively state whether the change is compensatory (i.e. a helpful way to maintain cardiac output in the face of ischemic heart disease) or decompensatory. This must be considered when interpreting findings in the aftermath of MI. For example, the Ca^{++} sensitivity increase could hypothetically serve as a short-term compensatory mechanism to maintain force generation capacity at all costs [33]. Alternatively, it could represent the beginnings of the heart's impaired relaxation rate and inability to respond to β-adrenergic stimulation by increasing heart rate that will ultimately be a characteristic feature of HF [24]. One could similarly concoct a reasonable explanation painting many of our other findings - including changes in cooperativity, decreased ATP consumption, phosphorylation changes, and disulfide protein oxidation – as either adaptive or maladaptive. In either case, our data add important information characterizing the post-MI/pre-remodeling phenotype. These data provide insights into both useful physiological responses to pathology and into the origins of the pathophysiological syndrome of HF.

Acknowledgements

We thank Dr. Marcelo Bonini for his helpful advice on assessing glutathionylation and Milana Grachoff for help with the echocardiography. .

This work was supported by American Heart Association-Midwest Pre-Doctoral Fellowship 2008-06682-00-00 (BSA) and by NIH Grants T32 007692 (BSA, KMS, SBS) and PO1 HL062426 (RJS, DLG, PHG).

References

[1] Rao VS, La Bonte LR, Xu Y, Yang Z, French BA, Guilford WH. Alterations to myofibrillar protein function in nonischemic regions of the heart early after myocardial infarction. Am J Physiol Heart Circ Physiol 2007; 293(1): H654-9.

[2] Layland J, Solaro RJ, Shah AM. Regulation of cardiac contractile function by troponin I phosphorylation. Cardiovasc Res 2005; 66(1): 12-21.

[3] Vahebi S, Ota A, Li M, Warren CM, de Tombe PP, Wang Y, Solaro RJ. p38-MAPK induced dephosphorylation of alpha-tropomyosin is associated with depression of myocardial sarcomeric tension and ATPase activity. Circ Res 2007; 100(3): 408-15.

[4] Seidman JG, Seidman C. The genetic basis for cardiomyopathy: from mutation identification to mechanistic paradigms. Cell 2001; 104(4): 557-67.

[5] Jacques AM, Copeland O, Messer AE, Gallon CE, King K, McKenna WJ, *et al*. Myosin binding protein C phosphorylation in normal, hypertrophic and failing human heart muscle. J Mol Cell Cardiol 2008; 45(2): 209-16.

[6] Biesiadecki BJ, Kobayashi T, Walker JS, Solaro RJ, de Tombe PP. The troponin C G159D mutation blunts myofilament desensitization induced by troponin I Ser23/24 phosphorylation. Circ Res 2007; 100(10): 1486-93.

[7] Kobayashi T, Dong WJ, Burkart EM, Cheung HC, Solaro RJ. Effects of protein kinase C dependent phosphorylation and a familial hypertrophic cardiomyopathy-related mutation of cardiac troponin I on structural transition of troponin C and myofilament activation. Biochemistry 2004; 43(20): 5996-6004.

[8] Keith M, Geranmayegan A, Sole MJ, Kurian R, Robinson A, Omran AS, Jeejeebhoy KN. Increased oxidative stress in patients with congestive heart failure. J Am Coll Cardiol 1998; 31(6): 1352-6.

[9] Sun, Y. Myocardial repair/remodelling following infarction: roles of local factors. Cardiovasc Res 2009; 81: 482-90.

[10] Cave AC, Brewer AC, Narayanapanicker A, Ray R, Grieve DJ, Walker S, Shah AM. NADPH oxidases in cardiovascular health and disease. Antioxid Redox Signal 2006; 8(5-6): 691-728.

[11] Doerries C, Grote K, Hilfiker-Kleiner D, Luchtefeld M, Schaefer A, Holland SM, et al. Critical role of the NAD(P)H oxidase subunit p47phox for left ventricular remodeling/dysfunction and survival after myocardial infarction. Circ Res 2007; 100(6): 894-903.

[12] Shiomi T, Tsutsui H, Matsusaka H, Murakami K, Hayashidani S, Ikeuchi M, et al. Overexpression of glutathione peroxidase prevents left ventricular remodeling and failure after myocardial infarction in mice. Circulation 2004; 109(4): 544-9.

[13] Jialal I, Devaraj S. Antioxidants and atherosclerosis: don't throw out the baby with the bath water. Circulation 2003; 107(7): 926-8.

[14] Canton M, Neverova I, Menabo R, van Eyk J, di Lisa F. Evidence of myofibrillar protein oxidation induced by postischemic reperfusion in isolated rat hearts. Am J Physiol Heart Circ Physiol 2004; 286: H870-H877.

[15] Prochniewicz E, Lowe DA, Spakowicz DJ, Higgins L, O'Connor K, Thompson LV, et al. Functional, structural, and chemical changes in myosin associated with hydrogen peroxide treatment of skeletal muscle fibers. Am J Physiol Cell Physiol 2008; 294(2): C613-C626.

[16] Sugden PH, Clark A. Oxidative stress and growth-regulating intracellular signaling pathways in cardiac myocytes. Antioxid Redox Signal 2006; 8(11-12): 2111-24.

[17] Sutton MG, Sharpe N. Left ventricular remodeling after myocardial infarction: pathophysiology and therapy. Circulation 2000; 101(25): 2981-8.

[18] Shioura KM, Geenen DL, Goldspink PH. Assessment of cardiac function with the pressure-volume conductance system following myocardial infarction in mice. Am J Physiol Heart Circ Physiol 2007; 293(5): H2870-7.

[19] Fabiato A. Computer programs for calculating total from specified free or free from specified total ionic concentrations in aqueous solutions containing multiple metals and ligands. Meth Enzymol 1988; 157: 378-417.

[20] Pagani ED, Solaro RJ. Methods for measuring functional properties of sarcoplasmic reticulum and myofibrils in small samples of myocardium.. Methods in Pharmacology (A. Schwartz, ed.) Vol. 5, Plenum Publishing Corp., N.Y. 1984; pp 44-61.

[21] Passarelli C, Di Venere A, Piroddi N, Pastore A, Scellini B, Tesi C, *et al*. Susceptibility of isolated myofibrils to in vitro glutathionylation: potential relevance to muscle functions. Cytoskeleton (Hoboken) 2010; 67(2): 81-9.

[22] Keller A, Nesvizhskii AI, Kolker E, Aebersold R. Empirical statistical model to estimate the accuracy of peptide identifications made by MS/MS and database search. Anal Chem 2002; 74(20): 5383-92.

[23] Nesvizhskii AI, Keller A, Kolker E, Aebersold R. A statistical model for identifying proteins by tandem mass spectrometry. Anal Chem 2003; 75(17): 4646-58.

[24] Solaro RJ, Westfall MV. Physiology of the Myocardium. In: Sellke FW, del Nido PJ, Swanson S, editors. Surgery of the chest. Philadelphia: Elsevier Saunders; 2005, pp. 767–79.

[25] Dalle-Donne I, Milzani A, Gagliano N, Colombo R, Giustarini D, Rossi R. Molecular mechanisms and potential clinical significance of S-glutathionylation. Antioxid Redox Signal. 2008; 10(3): 445-73.

[26] Christopher B, Pizarro GO, Nicholson B, Yuen S, Hoit BD, Ogut O. Reduced force production during low blood flow to the heart correlates with altered troponin I phosphorylation. J Muscle Res Cell Motil 2009; 30(3-4): 111-23.

[27] van der Velden J, Merkus D, Klarenbeek BR, James AT, Boontje NM, Dekkers DH, *et al*. Alterations in myofilament function contribute to left ventricular dysfunction in pigs early after myocardial infarction. Circ Res 2004; 95(11): e85-95.

[28] Li P, Hofmann PA, Li B, Malhotra A, Cheng W, Sonnenblick EH, *et al*. Myocardial infarction alters myofilament calcium sensitivity and mechanical behavior of myocytes. Am J Physiol 1997; 272(1 Pt 2): H360-70.

[29] Belin RJ, Sumandea MP, Kobayashi T, Walker LA, Rundell VL, Urboniene D et al. Left ventricular myofilament dysfunction in rat experimental hypertrophy and congestive heart failure. Am J Physiol Heart Circ Physiol 2006; 291(5): H2344-53.

[30] Hinken AC, Solaro RJ. A dominant role of cardiac molecular motors in the intrinsic regulation of ventricular ejection and relaxation. Physiology (Bethesda) 2007; 22: 73-80.

[31] Solaro RJ. Sarcomere control mechanisms and the dynamics of the cardiac cycle. J Biomed Biotech 2010 [in press]

[32] Alpert NR, Gordon MS. Myofibrillar adenosine triphosphatase activity in congestive heart failure. Am J Physiol 1962; 202: 940-6.

[33] Walker LA, Walker JS, Ambler SK, Buttrick PM. Stage-specific changes in myofilament protein phosphorylation following myocardial infarction in mice. J Mol Cell Cardiol 2010; 48(6): 1180-6.

[34] Clement O, Puceat M, Walsh MP, Vassort G. Protein kinase C enhances myosin light-chain kinase effects on force development and ATPase activity in rat single skinned cardiac cells. Biochem J 1992; 285 (Pt 1): 311-7.

[35] Chen FC, Ogut O. Decline of contractility during ischemia-reperfusion injury: actin glutathionylation and its effect on allosteric interaction with tropomyosin. Am J Physiol Cell Physiol 2006; 290(3): C719-27.

[36] Carpi A, Menabò R, Kaludercic N, Pelicci P, Di Lisa F, Giorgio M. The cardioprotective effects elicited by p66(Shc) ablation demonstrate the crucial role of mitochondrial ROS formation in ischemia/reperfusion injury. Biochim Biophys Acta 2009; 1787(7): 774-80.

[37] Heusch P, Canton M, Aker S, van de Sand A, Konietzka I, Rassaf T, Menazza S, Brodde OE, Di Lisa F, Heusch G, Schulz R. The contribution of reactive oxygen species and p38 mitogen-activated protein kinase to myofilament oxidation and progression of heart failure in rabbits. Br J Pharmacol 2010; 160(6): 1408-16.

[38] Evans CC, Pena JR, Phillips RM, Muthuchamy M, Wieczorek DF, Solaro RJ, Wolska BM. Altered hemodynamics in transgenic mice harboring mutant tropomyosin linked to hypertrophic cardiomyopathy. Am J Physiol Heart Circ Physiol 2000; 279(5): H2414-23.

[39] Chang AN, Harada K, Ackerman MJ, Potter JD. Functional consequences of hypertrophic and dilated cardiomyopathy-causing mutations in α-tropomyosin. J Biol Chem 2005; 280(40): 34343-9.

[40] Jagatheesan G, Rajan S, Schulz EM, Ahmed RP, Petrashevskaya N, Schwartz A, *et al*. An internal domain of beta-tropomyosin increases myofilament Ca(2+) sensitivity. Am J Physiol Heart Circ Physiol 2009; 297(1): H181-90.

[41] Andrade FH, Reid MB, Allen DG, Westerblad H. Effect of hydrogen peroxide and dithiothreitol on contractile function of single skeletal muscle fibres from the mouse. J Physiol. 1998 509 (Pt 2):565-75.

[42] Ambler SK, Hodges YK, Jones GM, Long CS, Horwitz LD. Prolonged administration of a dithiol antioxidant protects against ventricular remodeling due to ischemia-reperfusion in mice. Am J Physiol Heart Circ Physiol. 2008 295(3):H1303-H1310.

Table 1: Comparison of skinned fiber function between SH and MI

	SH (n = 16)	**MI (n = 14)**	***p*-value**
Max tension (*mN/mm*^{2})	21.8 ± 2.7	24.7 ± 2.4	N.S.
pCa_{50}	5.85 ± 0.01	5.89 ± 0.01	< 0.05
nH	3.80 ± 0.21	3.26 ± 0.13	< 0.05

The results of tension-pCa measurements of papillary skinned fibers are shown. Data comparing samples from sham-operated (SH) and post-myocardial infarction (MI) are given for maximum developed tension, pCa_{50} ($[Ca^{++}]$ producing 50% maximal tension development; a measure of calcium sensitivity) of each curve, and nH (slope of Hill equation). Numbers given represent sample mean ± SEM.

FIGURE LEGENDS

Fig. 1: Representative examples of echo cardiographic images and Evans Blue stain of SH and MI hearts

A. M-mode echo cardiographic images from sham-operated (SH) and post-myocardial infarction (MI) hearts were obtained at the mid-papillary level of the left ventricle. Analysis was performed 3 days post-surgery. Measurements showed significant left ventricular contractile function decline in post-MI animals. Line segments mark LV end-diastolic diameter (LVIDd) and end-systolic diameter (LVIDs). n = 4 SH, 6 MI

B. Hearts were stained with Evans blue dye and triphenyltetrazolium chloride (TTZ). Sections (1 mm thick) from SH and MI hearts are displayed sequentially (from base to apex going left to right). The "remote" zones that continued to receive blood flow after MI are stained blue. Red tissue represents viable tissue within the ischemic zone. White (unstained) tissue is irreversibly infarcted. Arrows indicate the left ventricular papillary muscles.

Fig. 2: Plot of the tension-pCa relation of papillary muscle "skinned fibers"

Data represent averaged tension at varying pCa values for detergent-extracted fiber bundles from non-infarcted left ventricular papillary muscles. MI fibers showed an increase in Ca^{++} sensitivity and a decrease in cooperativity of activation. n = 16 SH, 14 MI See Table 1 for data summary and analysis.

Fig 3: Histogram showing *in vitro* ATPase activity in ventricular protein samples

Myofibrillar protein extracts from SH (white) and MI (gray) hearts were homogenized and assayed for ATPase activity using a colorimetric assay for free PO_4 generation. Four different reaction solutions were used to measure myofilament actomyosin Mg-ATPase under relaxing (pCa ~8.0) and activating (pCa ~4.5) conditions, and myofilament myosin Ca-ATPase and K-ATPase. Results indicate that myofibrils from MI ventricles had diminished maximum actomyosin ATP hydrolysis attributable to an alteration in myofibrillar myosin ATPase. Units given in nmol PO_4/mg protein/min n = 22 (Mg-ATPase relaxing and activating), 20 (Ca-ATPase), 12 (K-ATPase) * statistically significant difference between SH and MI

Fig 4: Gel and histogram showing net phosphorylation status of cTnI in papillary samples

A. Myofilament proteins from skinned fibers dissected from the viable portions of detergent-extracted papillary muscles from SH and MI hearts were separated by SDS-PAGE. Levels of phosphorylation were determined by ProQ Diamond Phosphoprotein Stain, and the gel was stained with Coomassie Blue to visualize total protein loading. The leftmost lane is a molecular mass standard (DualColor; BioRad) with bands corresponding to the indicated masses in kD; sample lanes are labeled as MI (M) or SH (S). A duplicate molecular mass standard has been cropped from the right side of each image.

B. Histogram depicting the data from A. Values for protein phosphorylation in SH (white) and MI (gray) samples represent arbitrary units defined by ratios of protein phosphorylation normalized for abundance of actin. Sarcomeric proteins listed are myosin binding protein C (MyBP-C), desmin, cardiac troponin T (cTnT), tropomyosin (Tm), cardiac troponin I (cTnI), and myosin light chain 2 (MLC2). cTnI and MLC2 phosphorylation was ~20% lower in MI samples. n = 5 * statistically significant difference between SH and MI

Fig 5: Representative non-reducing/reducing "diagonal gel" showing Tm oxidation

A. Myofilament fraction homogenates from ventricular tissue were separated by SDS-PAGE under non-reducing and reducing conditions, and stained with Coomassie Blue to visualize the proteins. Reduction-sensitive putative disulfide products appear to the left of the diagonal in each protein sample. The circled spot represents an oxidized product containing Tm. Tm oxidation was higher in the MI sample in 7 out of 8 pairings from sarcomeric fractions of whole-ventricles and in 7 out of 9 pairings from viable papillary skinned fiber samples.

B. Putative oxidized Tm products from the experiment series shown in A. were subjected to LC-MS/MS analysis. Peptides were analyzed on an LTQ-FT-ICR instrument equipped with a capillary column and nanospray source. α-tropomyosin was identified with high confidence (100% protein probability) in an analysis of 13 unique peptides, 18 unique spectra, and 39 total spectra; 99/284 amino acids were represented in the analysis for 35% sequence coverage of the protein. Shown above the spectra is the sequence coverage of Tm with peptides in yellow. MS/MS spectra of doubly charged m/z 657.89 ion,

corresponding to Tm peptide 168-178 (KLVIIESDLER), are shown in the lower portion. Tm was the only protein confidently identified in 4 out of 4 MI samples.

Fig 6: Western blot and histogram depicting protein glutathionylation

A. Western blot (left) and Ponceau stain (right) comparing SHAM (S), MI (M), positive control (+; reduced glutathione and diamide), and negative control (-; DTT) samples. Myofilament fraction homogenates prepared with NEM were subjected to SDS-PAGE/Western analysis and probed with an anti-glutathione antibody. Membranes were stained with Ponceau S to normalize for total protein loading. **B.** Histogram representation of the results of A. Glutathionylation of sarcomeric proteins is higher after MI. n = 6 SH, 4 MI * statistically significant difference between SH and MI

Fig 7: Before-after plots showing the effect of a reducing agent on Ca^{++} sensitivity in papillary "skinned fibers"

Tension-pCa relations were obtained for non-infarcted fiber bundles from detergent-extracted papillary muscles over two contraction series. Prior to the second set of measurements, each fiber was treated with 0.1 M DTT for 10 min. DTT treatment did not significantly alter Ca^{++} sensitivity in SH fibers, but reduced Ca^{++} sensitivity in MI samples. Values represent paired measurements of non-reduced and reduced pCa_{50} value for each fiber. n = 7 SH, 9 MI SH p N.S., MI $p < 0.005$ Unpaired sample means ± SEM are SH: 5.82 ± 0.02 before, 5.82 ± 0.02 after; MI: 5.87 ± 0.03 before, 5.84 ± 0.02 after. ΔpCa_{50} means are SH 0.01 ± 0.01, MI 0.03 ± 0.01, $p < 0.05$. Samples whose ΔpCa_{50} deviated by > 2 S.D. were excluded from the analysis.

Figure 1

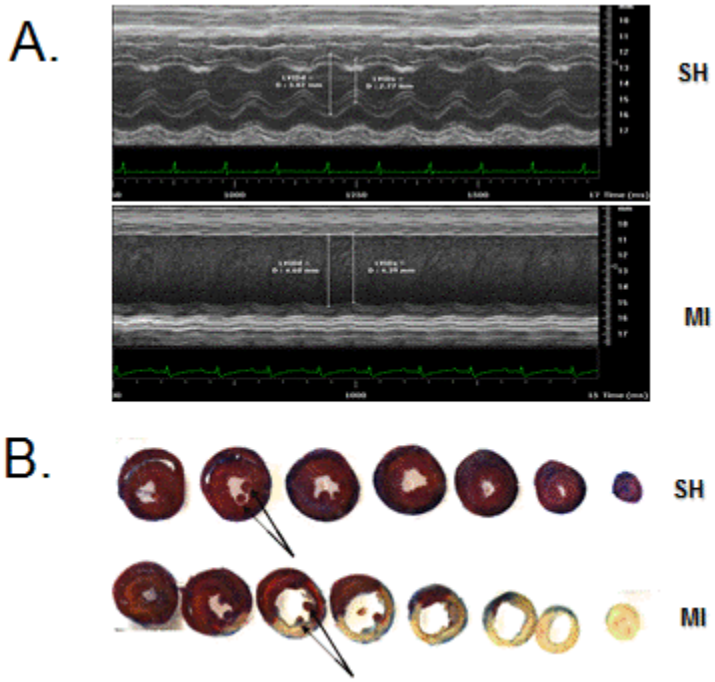

Figure 2

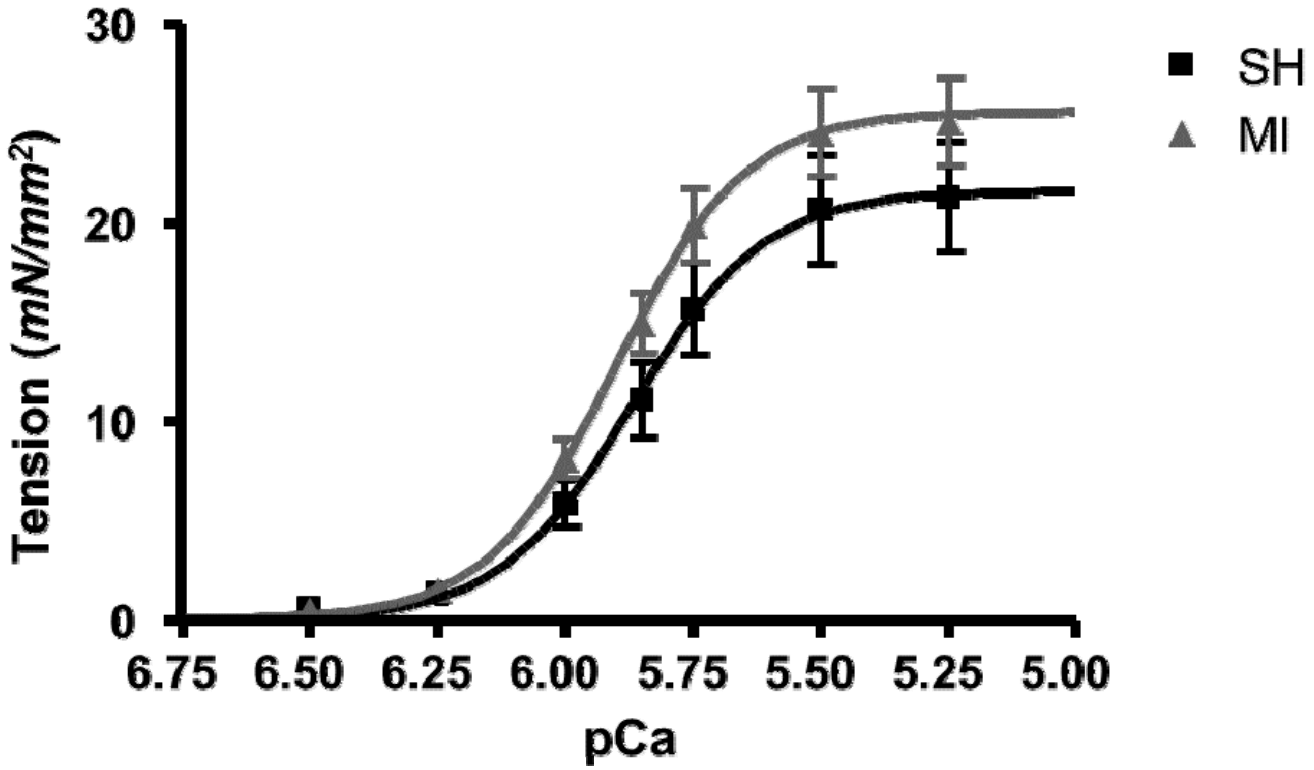
30
20
10
0
Tension (mN/mm²)
6.75
6.50
6.25
6.00
5.75
5.50
5.25
5.00
pCa
SH
MI

Figure 3

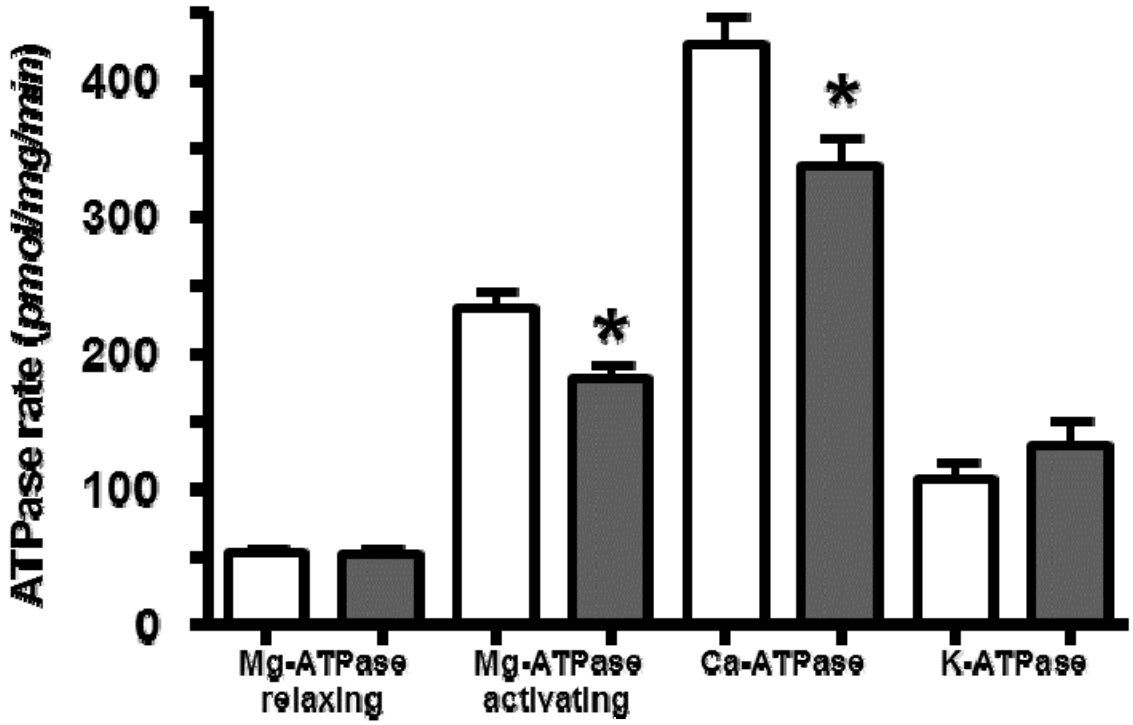
ATPase rate (μmol/mg/min)
400
300
200
100
0
*
*
Mg-ATPase relaxing
Mg-ATPase activating
Ca-ATPase
K-ATPase

Figure 4

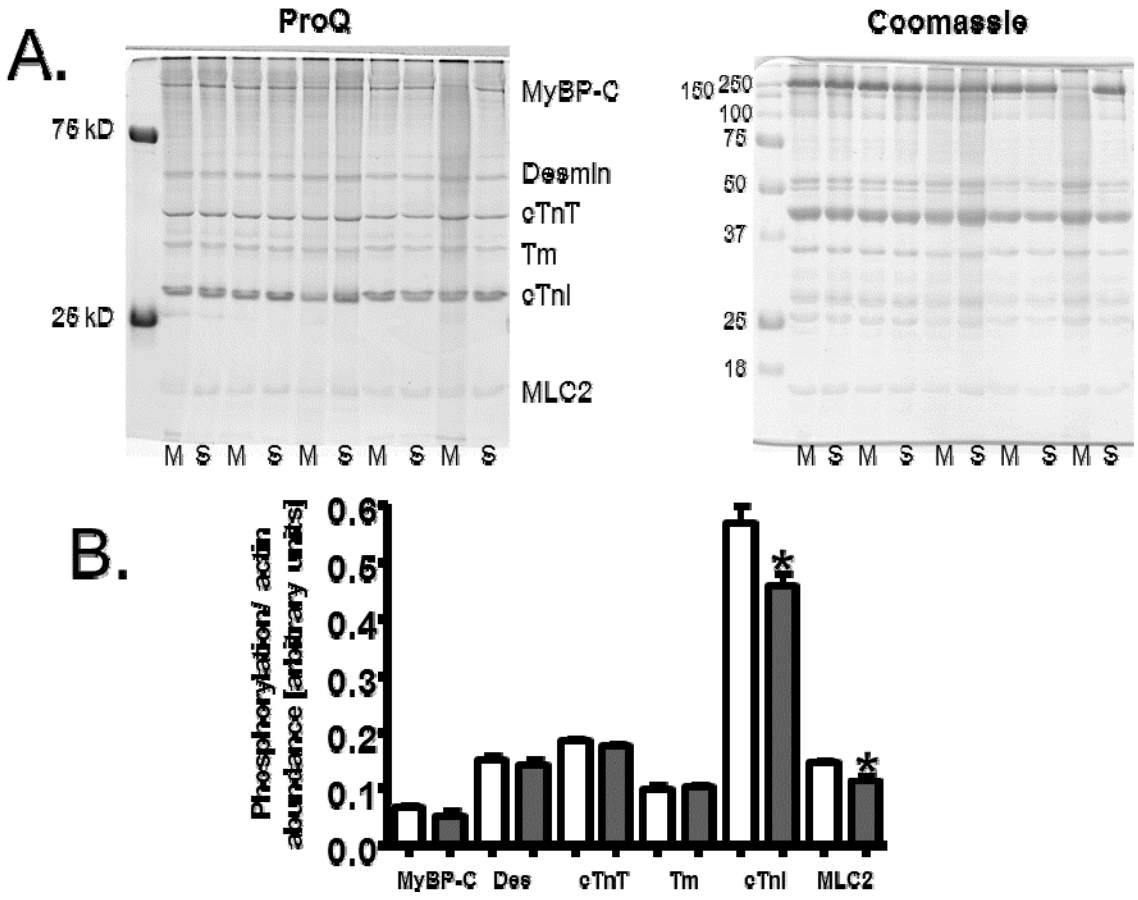
A.
ProQ
Coomassie
75 kD
25 kD
MyBP-C
Desmin
cTnT
Tm
cTnI
MLC2
150
250
100
75
50
37
25
20
M S M S M S M S M S
M S M S M S M S M S
B.
Phosphorylation/ actin abundance [arbitrary units]
0.6
0.5
0.4
0.3
0.2
0.1
0.0
MyBP-C
Des
cTnT
Tm
cTnI
MLC2

Figure 5

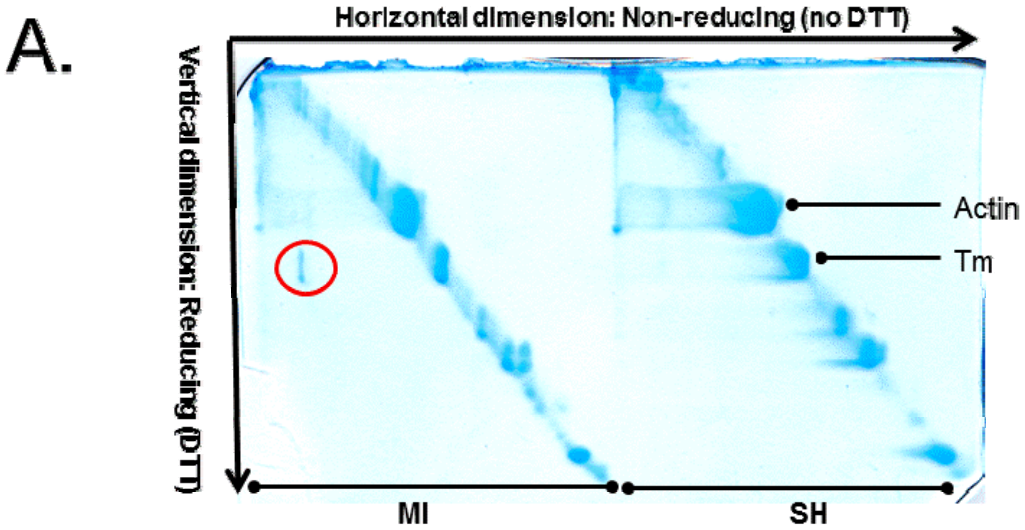
A.
Horizontal dimension: Non-reducing (no DTT)
Vertical dimension: Reducing (DTT)
Actin
Tm
MI
SH

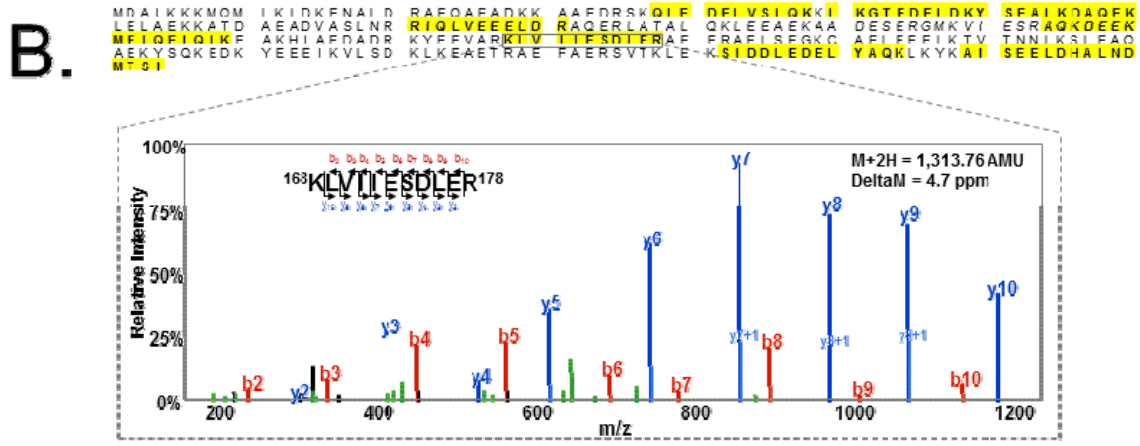
B.
163KLVILESDLER178
M+2H = 1,313.76 AMU
DeltaM = 4.7 ppm
Relative Intensity
100%
75%
50%
25%
0%
200
400
600
800
1000
1200
m/z

Figure 6

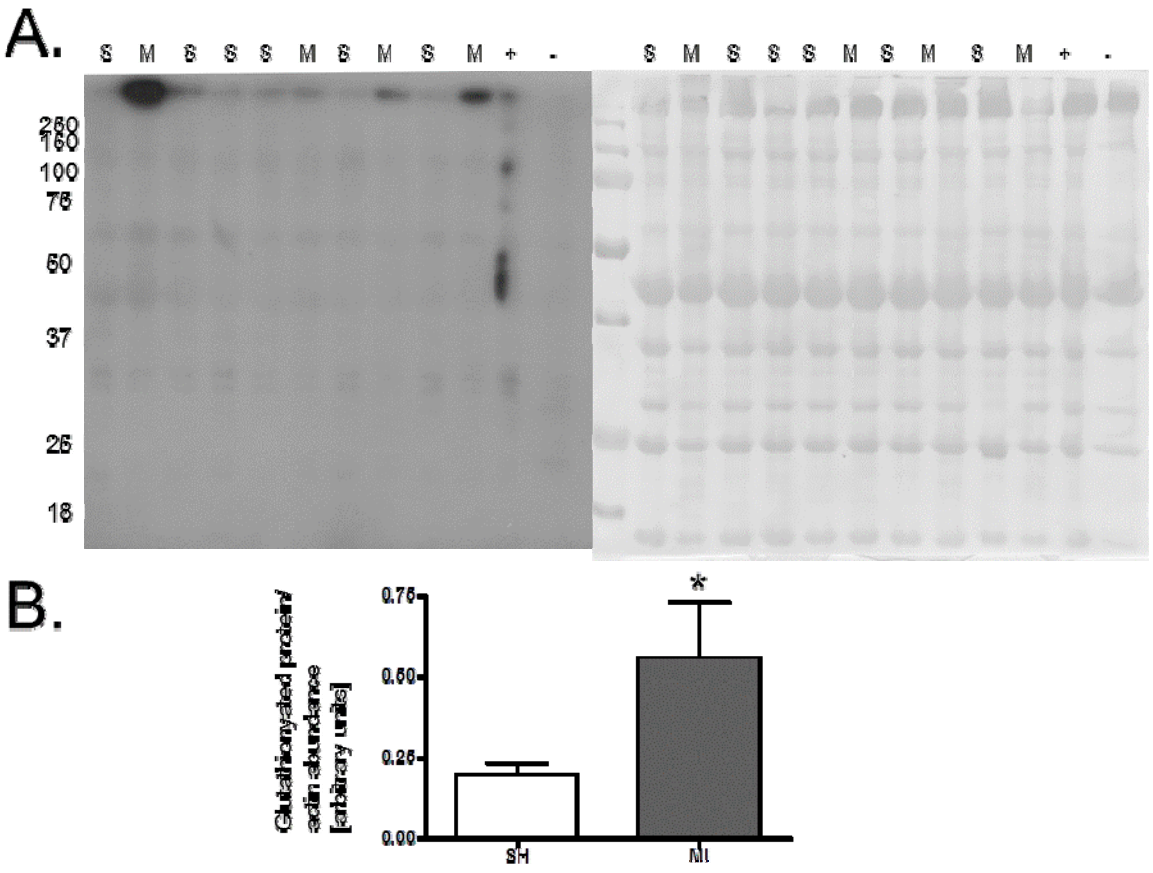
A.
S M S S S M S M S M + -
S M S S S M S M S M + -
250
150
100
75
50
37
25
18
B.
Glutathionylated protein/
actin abundance
[arbitrary units]
0.75
0.50
0.25
0.00
*
SH
MI

Figure 7

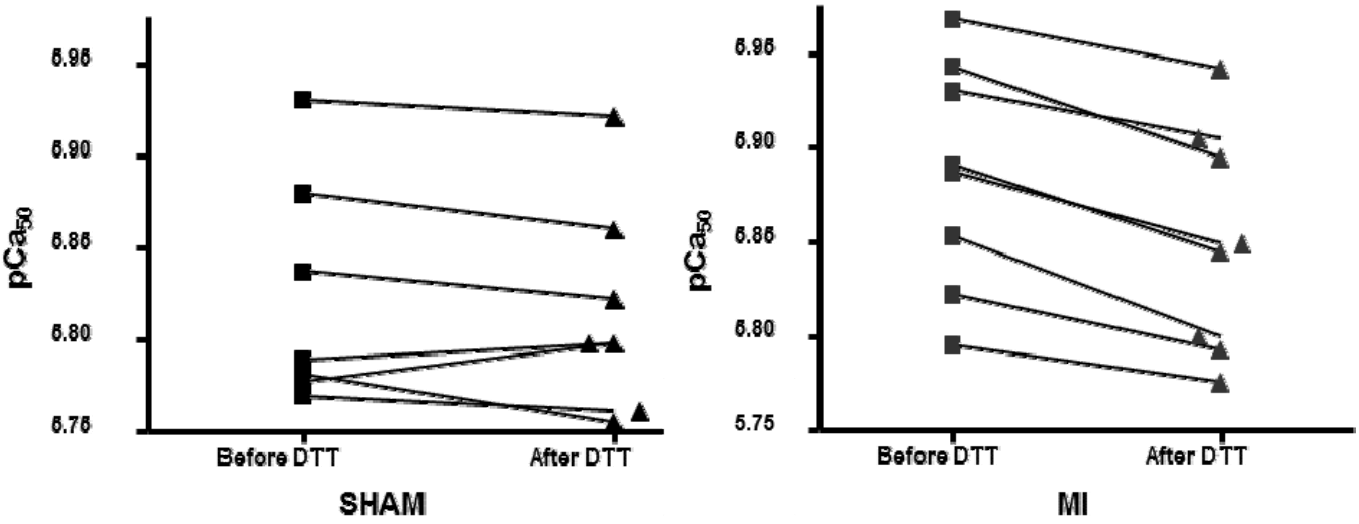
6.95
6.90
6.85
6.80
6.75
pCa50
Before DTT
After DTT
SHAM
6.95
6.90
6.85
6.80
6.75
pCa50
Before DTT
After DTT
MI